

High Capacity Image Steganography in Wavelet Domain

D.Lakshmi NarayanaAssociate Professor,
Department of ECE,
A.I.E.T, Narisipatnam,
Visakhapatnam.**K.S.Guru Murthy**Assistant Professor,
Department of ECE,
A.I.E.T, Thagarapavalasa,
Visakhapatnam.**B.Ravi Kiran**Assistant Professor,
Department of ECE,
A.I.E.T, Thagarapavalasa,
Visakhapatnam.**V.Suresh**Assistant Professor,
Department of ECE,
A.I.E.T, Thagarapavalasa,
Visakhapatnam.

Dwarapunari6@gmail.com

Abstract:

A new high capacity method for transform domain image steganography is introduced in this paper. The proposed steganography algorithm works on the wavelet transform coefficients of the original image to embed the secret data. As compared to current transform domain data hiding methods, this scheme can provide a larger capacity for data hiding without sacrificing the cover image quality. This is achieved through retaining integrity of the wavelet coefficients at high capacity embedding. This improvement to capacity-quality trading-off interrelation is analyzed in detailed and experimentally illustrated in the paper.

I.INTRODUCTION:

Information hiding has attracted lots of attention over recent years. It is the art and technique of concealing a message in a cover without leaving any remarkable trace on the cover signal [1]. There are three main compromising attributes for a data hiding system, known as capacity, imperceptibility, and robustness. The data hiding schemes are principally categorized into steganography and watermarking, according to the application based requirements. In the steganography systems, our goal is to provide more capacity, where a better robustness characteristic is of concern in watermarking. The capacity requirements are often satisfied with techniques in spatial domain, where transform domain techniques provide higher robustness against changes and attacks. Accordingly, majority of non-fragile watermarking algorithms use transform domain techniques because of their critical need for robustness, while spatial domain hiding methods are more attractive in steganography schemes due to the capacity concerns. Despite this general trend, the vast use of the compressed images over the internet and in most multimedia communications have encouraged researchers to challenge the issue of hiding capacity in transform domains, e.g. DCT (Discrete Cosine Transform) and wavelet transforms, for image steganography. This is the main theme of the current paper. JPEG2000, which is a recent image

compression standard, utilizes the wavelet transform. In addition to two general benefits for transform domain techniques mentioned above, the wavelet transform has the additional advantage of being more compatible with the HVS (Human Visual System). Therefore, there is an increasing tendency to developing information hiding algorithms in wavelet domain. These methods, as mentioned earlier, have a limited capacity and are more suitable for image watermarking [2-4]. However, there are few steganography schemes developed in wavelet domain. For example, El-Khamy et al. offered a steganography method combining wavelet transform and fractal image coding in [5]. Hay-ying et al. introduced an algorithm that concealed the message directly in the JPEG2000 compressed bit-stream [6]. However, none of these methods could outperform the method proposed by Ramani et al. in [7], in terms of the embedding capacity. This is while our proposed steganography method provides a hiding capacity, up to two times of the capacity given by the Ramani's technique, without sacrificing the stego image quality. This paper is organized as follows. Section II details our proposed algorithm. Section III presents the experimental results that are discussed and compared to the results obtained from using the Ramani's method in section IV. Section V concludes the paper.

II.PROPOSED ALGORITHM:

A.Wavelet transform:

The proposed scheme uses the wavelet transform presentation of the cover image to conceal the secret message. In a four-band two-dimensional wavelet transform, the LL band includes the low pass coefficients and represents a soft approximation to the image. The HL, LH and HH bands represent the vertical, horizontal, and diagonal features of the image, respectively. These three bands convey the details of the image. We can do the same decomposition on the LL quadrant up to $\log_2(\min(\text{height}, \text{width}))$. Figure 1 visualizes a two-level wavelet transform. The 2D wavelet transform used in this algorithm is the integer wavelet transform introduced in [9], the same transform used in [7].

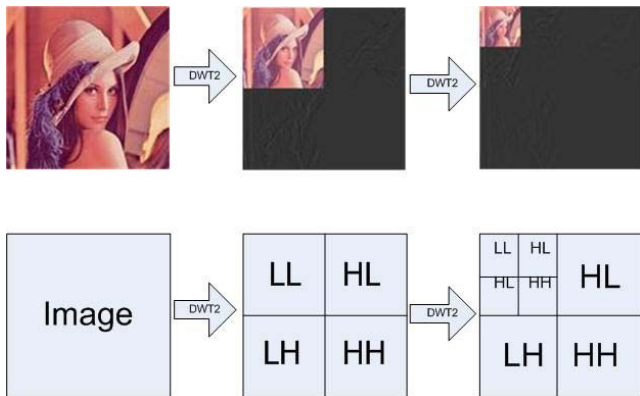


Figure 1. 2-level 2D wavelet transform

B.Bit Plane Complexity Segmentation:

Generally, wavelet domain allows for hiding data in regions that the HVS is less sensitive [10]. To do this, we adapt the amount of embedded data in each region of wavelet transform domain with a measure of noisiness in that region. Here, we use the bit-plane complexity segmentation (BPCS) [8] as the measure of noisiness. Each RGB component of a 24-bit bitmap image is an 8-bit value that changes from 0 to 255. In each color plane, the value zero represents the darkest shade of that color, where the brightest shading corresponds to the 255 value. Figure 2 shows a 4*4 test image with the RGB values shown in Table I. Therefore, the R channel is decomposed as indicated in Table II. Now, the bit plane segmentation, visualized in Figure 3, results in eight binary planes for R channel, as shown in Table III. As a benchmark to measure the amount of noisiness of a bit plane, we use the black and white border image complexity defined by Kawaguchi [8]. Based on the definition, the complexity for a black and white border P (equivalent to our segmented plane) is the ratio of the number of total B-W changes in the plane to its maximum possible value, denoted as $\alpha(P)$, where $0 < \alpha(P) < 1$.



Figure 2. Test image

TABLE I. RGB VALUES FOR TEST IMAGE:

R	1	2	3	4	G	1	2	3	4	B	1	2	3	4
1	175	39	80	202	1	247	223	9	69	1	9	247	247	252
2	167	30	80	190	2	225	206	30	32	2	30	225	255	251
3	164	38	91	165	3	217	199	38	4	3	38	217	217	255
4	155	35	85	134	4	197	169	35	3	4	29	184	201	184

TABLE II. BINARY REPRESENTATION OF R CHANNEL

10101111	00100111	01010000	11001010
10100111	00011110	01010000	10111110
10100100	00100110	01011011	10100101
10011011	00100001	01010101	10000110

TABLE III. BINARY PLANES FORM R CHANNEL

Plane 8	Plane 7	Plane 6	Plane 5
1 0 0 1	0 0 1 1	1 1 0 0	0 0 1 0
1 0 0 1	0 0 1 0	1 0 0 1	0 1 1 1
1 0 0 1	0 0 0 0	1 1 0 1	0 0 1 0
1 0 0 1	0 0 1 0	0 1 0 0	1 0 1 0
Plane 4	Plane 3	Plane 2	Plane 1
1 0 0 1	1 1 0 0	1 1 0 1	1 1 0 0
0 1 0 1	1 1 0 1	1 1 0 1	1 0 0 0
0 0 1 0	1 1 0 1	0 1 1 0	0 0 1 1
1 0 0 0	0 0 1 1	1 0 0 1	1 1 1 0

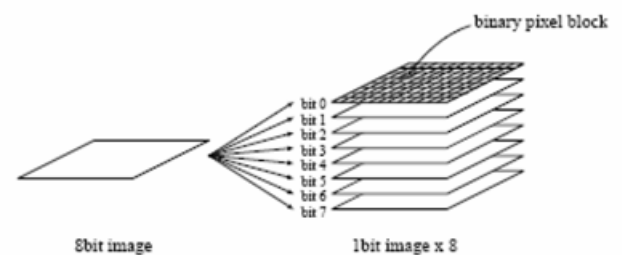


Figure 3. Decomposition of block to binary planes

Following measuring the complexity of each plane, we compare the complexity to a threshold to decide if it is a noisy plane. This threshold is to compromise between capacity and imperceptibility. We segment each channel of wavelet transform representation into 8*8 blocks with pixel values changing from 0 to 255. For each block, we construct the relevant 8-bit planes and compare the bit plane complexity with threshold from the MSB bit plane to the LSB bit plane.

Once the first plane with a complexity higher than the threshold is found, we decide on the number of bits that can be embedded in the block pixels. As an example, we can embed five bits of message in the five LSBs of each pixel of the block, if the fourth plane is the first one with a complexity higher than the threshold. For each RGB channel, the threshold is adjusted adaptively according to:

$$C_{th} = C_{in} \times C_{max} \quad (1)$$

where C_{in} is the parameter to compromise between capacity and imperceptibility ranging from zero to one, C_{max} denotes the maximum complexity in the relevant channel, and C_{th} is the comparative threshold used for making decision on the planes of that channel.

C.Algorithm:

We segment the wavelet representation of the image into 8×8 blocks and determine the capacity of each block, in terms of bit per pixel, using the BPCS. A random seed is used to determine the order of conveying blocks. For each block, the red, green, and blue channels are used for the message bit embedding. The pseudorandom generator is initialized using a session key, agreed between transmitter and receiver. The embedding rule is so simple: the pixel value is changed into the nearest integer with the last LSB bits equal to the input bits. For example, assume that capacity of the current block is found to be 3 bits. Then, the current pixel is equal to 17 or (00010001)_b and the input bits are equal to (100)_b. According to the rule described above, the value of pixel is changed into 20 or (00010100)_b. In the same case, with the input equal to (110)_b, the turned value of the pixel is 14 or (00001110)_b. And, in the case of input equal to (101)_b, there is no preference for choosing 13 or 21, as the output value. The embedding rule is simply described as:

$$y = x + A \times (A \leq B) - B \times (B < A) \quad (2)$$

where

$$\begin{aligned} A &= \text{mod}(m - x, 2^c) \\ B &= \text{mod}(x - m, 2^c) \end{aligned} \quad (3)$$

and x , m , c , and y stand for pixel value, input value, capacity, and output value, respectively. There are two exceptions in the embedding algorithm discussed above. The first one is about the first pixel of each block that is used to convey the capacity, with a 3-bit input indicating the block's capacity changing from 0 to 7. These three bits suffice to bear the amount of capacity, because the MSB plane would never change even for very low thresholds.

The next exception applies to the planes with capacity equal to 1, where we use a specific embedding method described in section IV. Applying the abovementioned rules to the sender end, ensures us to extract the message in the receiver end based on the equation below, where c , y , and m denote capacity, pixel value, and extracted message bit, respectively.

$$m = \text{mod}(y, 2^c) \quad (4)$$

The embedding and the extracting algorithms are detailed in the following:

Embedding:

1. Compute the 2D wavelet transform of the image and segment it into 8×8 blocks.
2. Use the secret key to determine the order of blocks selected for embedding.
3. Find the maximum complexity of blocks of each channel and, hence, the appropriate complexity threshold for that channel.
4. Determine the capacity of each block finding its first MSB plane possessing a complexity higher than the threshold.
5. Embed the capacity of the block in its first pixel using (2) and (3) with $c=3$ and $m=\text{capacity}$.
6. If the capacity is not equal to 1, embed the input bits of the block capacity in its remaining pixels using (2) and (3). Otherwise, change the pixels such that to satisfy (7) using the method in [11].
7. Generate the stego image by computing the inverse 2D wavelet transform.

Extracting:

1. Compute the 2D wavelet transform of the image and segment it into 8×8 blocks.
2. Use the secret key to determine the order of blocks selected for embedding.
3. Extract the capacity of blocks using (4) with c equal to 3 from the first pixel of the block.
4. Extract the message bits using (4) with c equal to the capacity extracted in step 3, if c is not equal to one; otherwise, use (7) for extraction.

III.EXPERIMENTS AND RESULTS:

The 256×256 24-bit bitmap RGB colored Lena image is selected as subject of our experiments to compare the

performance of our method to that of the Ramani's method [7]. The latter algorithm uses the same complexity criterion and the same relation for finding the channel thresholds as those we have used in our method (equation 1). Therefore, we can compare the capacity and the image quality obtained using the same threshold in both methods. The corresponding curves are shown in figures 4 and 5. The image quality is measured in terms of the PSNR. From Figure 4, it is clear that our algorithm provide higher capacity with the same C_{in} parameter selected for both algorithms. This difference, in average, provides about one bit per pixel additional embedding capacity in our cover image which is equal to $256 * 256$ bits (about 8 Kbytes). Figure 5 gives a comparison of the received PSNR for both methods using the same C_{in} parameter. As shown, our algorithm results in a higher stego image quality, in the sense of the PSNR, as compared to the reference algorithm, despite the larger number of bits embedding in our method.

This improvement is about 2.5dB in average, in terms of the PSNR. In the case of the same embedding capacity, this mean difference is about 3 dB, due to figure 6. In this case, we calculated the capacity for Ramani's algorithm at different thresholds, and then embedded the same amount of data into the image using both algorithms. Figure 7, derived heuristically, presents the capacities provided by the two algorithms at the same image quality in terms of the PSNR. It means that for each PSNR and capacity attained from the Ramani's algorithm, we have tried our algorithm with several C_{in} 's to find a case with almost the same PSNR. Taking the PSNR margin of 36dB as the HVS noticeable distortion, it can be inferred from figure 6 that we can embed up to about 6 bits per pixel (about 48 Kbytes) for a $256 * 256$ 24-bit bitmap image, without a noticeable distortion, using the proposed method. This is while

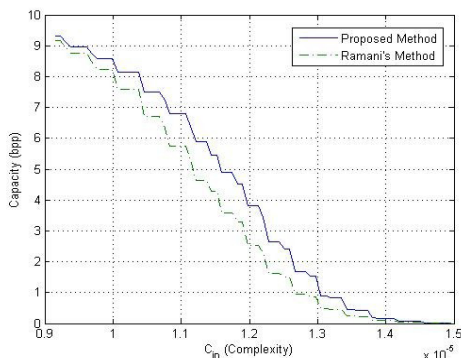


Figure 4. Capacity versus complexity threshold for both methods

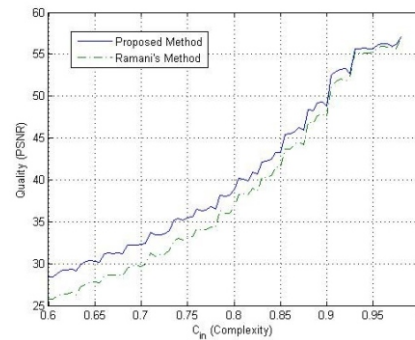


Figure 5. PSNR versus complexity threshold for both

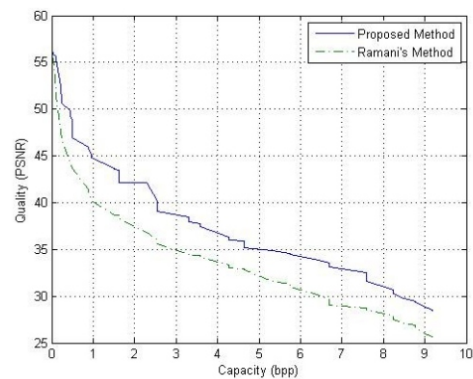


Figure 6. PSNR versus capacity for both methods

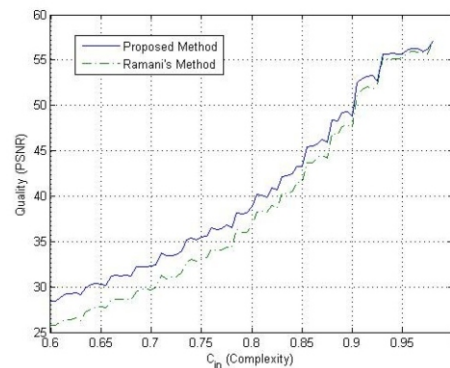


Figure 7. Capacity versus PSNR for both methods

TABLE IV BPP AND PSNR COMPARISON FOR FOUR IMAGES AND BOTH METHODS

		Baboon		F16		Peppers		Woman	
		Pro.	Ram.	Pro.	Ram.	Pro.	Ram.	Pro.	Ram.
0.3	bpp	15.1	15.1	11.8	11.7	12.1	12.1	12.6	12.5
	PSNR	18.4	15.5	20	18	20.1	17.6	21.7	19
0.4	bpp	14.4	14.4	10.7	10.6	11	10.9	11.5	11.5
	PSNR	19.6	16.5	21.7	19.3	22.1	19.6	24.7	21.9
0.5	bpp	13.5	13.4	9.4	9.4	9.7	9.7	10.5	10.5
	PSNR	21.6	18.5	24.4	21.7	25.1	22.5	27.1	24.5
0.6	bpp	12.3	12.1	8.3	8.2	8.5	8.4	9.4	9.2
	PSNR	24.3	21.5	27.1	24.3	28.3	25.7	29.6	26.9
0.7	bpp	10	8.1	6.6	6.1	6.8	6.3	6.3	4.9
	PSNR	28.9	25.3	32	29	33.1	30	35.8	32.4
0.8	bpp	4	2	3.4	2.3	3.6	2.5	1.8	1
	PSNR	37.8	33.2	38.8	35.4	41.3	36.4	43.7	40
0.9	bpp	0.3	0.1	0.5	0.2	0.5	0.3	0.1	0
	PSNR	51	45.2	51.7	45.9	51.8	48.3	56.3	52.4

the same HVS margin corresponds to about 22.4 Kbytes in the Ramani’s method. Table IV represent the comparative results for four other famous pictures. This illustration confirms that we have improved both capacity and imperceptibility, or indeed their trading-off margins, as one of major issues in image steganography. This improvement is discussed in more detail in the next section.

IV. ANALYSIS AND DISCUSSION:

We mentioned in Section III that we significantly improved both the embedding capacity and quality of the stego image simultaneously. These improvements are achieved using some key features of the two embedding approaches: our own method and the Ramani’s scheme. In this section, we discuss about the reasons for these major improvements in detail.

A. Capacity:

Both algorithms start with three common steps of the embedding process, as mentioned in Section II, but take difference steps as of the step 4. We index the MSB and the LSB planes of a block with 8 and 1, respectively, where the middle planes are indexed accordingly. In the Ramani’s method, every complex plane is replaced with a bit plane from message. Assuming that the planes 4 and 1 are recognized as the complex planes in a block, we then have the block conveying only 2x64=128 bits. Basically, we are not allowed for making any changes to plane 2 or 3 here.

Also, the replacing message plane should be complex to be identified as a conveying plane in the retrieval process. Henceforth, we may need to conjugate [8] the message plane to be complex if it is not. It means that we need to store a conjugation map beside the message. This is not the case in our method; therefore we do not need such a map, because we get the capacity of each block inside the same block. We can also change the four planes in this example, according to our embedding method, without concerning about uniqueness of the retrieving process. So, we have a capacity of 4x63=252 bits in this block. It is observed that several cases like this example happen in our experiments, making possible such a significant improvement on the capacity.

B. Imperceptibility:

Let’s assume that we deal with a case where all c LSB planes of a block are recognized as complex planes. In other words, we are ignoring the capacity difference between the two methods. We observe a pixel in this block and suppose that c is not equal to one. Following replacement of the c planes with the message planes, the expectation of the change of pixel value will be equal to c_{old} , as:

$$c_{old} = \frac{\sum_{i=1}^{2^c} \sum_{j=1}^{2^c} abs(i-j)}{2^{2c}} = \frac{2^c \times \sum_{i=1}^{c-1} 4^i}{2^{2c}} = \frac{4^c - 1}{3 \times 2^c} \quad (5)$$

The equality can be derived with breaking the summation on j into two summations, where the first part changes from 0 to i and the second part varies from $i+1$ to 2^c . Now, we calculate a similar parameter for our method, called c_{new} . The main difference here is that, in our method, it is not possible for a value to change more than $2c-1$ times. Therefore, the expected change in each pixel value in this case is given as:

$$c_{new} = \frac{\sum_{i=1}^{2c-1} abs(i-2^{c-1})}{2_c} = \frac{4^{c-1} - 2^{c-2}}{2_c} \quad (6)$$

A comparison between these two parameters is depicted in figure 8. Hence, the average change per wavelet coefficient has a lower value in our method, so the coefficients remain more intact in our method with certain capacity of data embedded. This, results in more intact image pixels and consequently a higher stego image quality.

This is simply deduced from both the equations and figure 8 that, in case of $c=1$, the average probability of change is equal to $1/2$ in the both methods. This is the reason why we use the other method for embedding the message in planes with $c=1$. The first pixel of block is preserved to store the capacity, so there are 63 more pixels left. This algorithm takes three input pixels x_1, x_2 and x_3 and three message bits m_1, m_2 and m_3 and generates the changed outputs values y_1, y_2 and y_3 as:

$$\begin{aligned} m_1 &= LSB(y_1 + \lfloor y_2 / 2 \rfloor) \\ m_2 &= LSB(y_2 + \lfloor y_3 / 2 \rfloor) \\ m_3 &= LSB(y_3 + \lfloor y_1 / 2 \rfloor) \end{aligned} \quad (7)$$

The procedure is repeated 21 times for each block with $c=1$. This embedding algorithm is called One-third probability algorithm and it is shown here that the probability of change per pixel decreases from $1/2$ to $1/3$ [11].

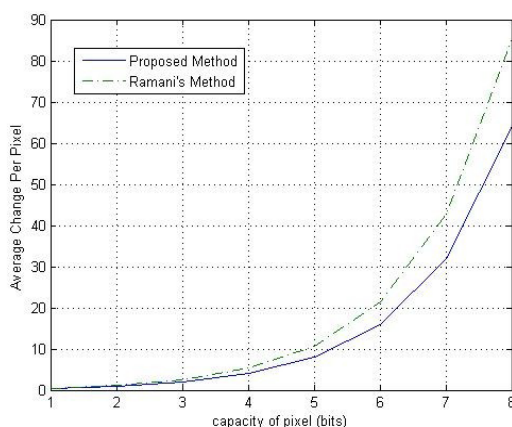


Figure 8. Average change per pixel comparison between both methods

V.CONCLUSION:

We have introduced a new high capacity steganography method in wavelet domain. In order to achieve a higher quality of the stego image, we firstly estimate the capacity of each DWT block using the BPCS. The embedding process is then performed over the whole block, rather than in its bit-planes. This approach to the embedding ensures that no noisy bit-plane is left unused. Therefore, we achieve a much greater capacity as compared to that offered by previous methods, as confirmed by our analysis and experiments. The proposed approach to the embedding process may also be extended to other transform domains to improve the compromising interrelation between capacity and imperceptibility in image steganography.

REFERENCES:

- [1] D. Artz, "Digital steganography: hiding data within data," IEEE Internet Computing, pp.75-80, May-June 2001.
- [2] L. Sunil, C.D.Yoo, T.Kalker, "Reversible Image Watermarking Based on Integer-to-Integer Wavelet Transform", IEEE Transaction of information, forensics and security, September 2007.
- [3] T. G. Gao, Q. L. Gu, "Reversible watermarking algorithm based on wavelet lifting scheme," Wavelet analysis and pattern recognition conference, November 2007.
- [4] N. Bi, Q. Sun, D. Huang, Z. Yang and J. Huang, "Robust watermarking based on multiband wavelets and empirical mode decomposition," IEEE transaction on image processing, August 2007.
- [5] S. E. El-Khany, M. Khedr, A. AlKabbany, "A hybrid fractal-wavelet data hiding technique" 25th NRCS, March 2008.
- [6] G. Hay-ying, X. Yin, L. Xu and L. Guo-qiang, "A steganographic algorithm for JPEG2000 image," Conference on computer science and software engineering, 2008.
- [7] M. K. Ramani, E. V. Prasad, S. Varadarajan, "Steganography using BPCS to the integer wavelet transformed image" IJCSNS, July 2007.
- [8] E. Kawaguchi and R. O. Eason, "Principle and application of BPCS- steganography," in Proc. SPIE, vol 3529, pp 464-473, 1998.
- [9] A. R. Calderbank, I. Daubechies, W. Sweldens and B. Yeo., "Wavelet transforms that map integers to integers". Applied and Computational Harmonic Analysis, vol.5, noJ, pp.332-369, 1998.
- [10] R. O. El Safy, H.H. Zayed, A. El Dessouki, "An adaptive steganographic technique based on integer wavelet transform," 2009.
- [11] S. Sarreshtedari, M. Ghotbi, S. Ghaemmaghami, "One-third probability embedding: less detectable steganography," IEEE International conference on multimedia and expo, July 2009.